Magnetic force microscopy and simulations of colloidal iron nanaparticles

Magnetic force microscopy and simulations of colloidal iron nanoparticles

F. Pedreschi[a)]
School of Physics, Dublin Institute of Technology, Kevin Street, Dublin 8, Ireland

J. M. Sturm
Department of Physics, Eindhoven University of Technology, 5600MB, Eindhoven, The Netherlands

J. D. O'Mahony
School of Physics, Dublin Institute of Technology, Kevin Street, Dublin 8, Ireland

C. F. J. Flipse
Department of Physics, Eindhoven University of Technology, 5600MB Eindhoven, The Netherlands

(Received 27 August 2002; accepted 28 May 2003)

Colloidal iron nanoparticles with a core size of 10.6 nm were examined using magnetic force microscopy. Surprisingly, single nanoparticles were more prominently visible in magnetic force gradient images than clusters. A simple qualitative model is proposed to explain this observation, speculating that the local field produced by a cluster of particles may be sufficient to align their moments in the plane of the cluster, even though the particles are superparamagnetic. An alternative possibility of spin glass formation within clusters is also considered. Calculations performed with nanoparticles represented as single dipoles appear to match experimental data quite well. © *2003 American Institute of Physics.* [DOI: 10.1063/1.1593219]

I. INTRODUCTION

Metallic magnetic nanoparticles have recently been attracting a great deal of experimental and theoretical interest due to their potential use in practical applications such as magnetic storage and ''spintronic'' devices[1] and because they represent, in many ways, an intermediate state of matter between bulk and atom. With regard to magnetic data storage in particular, an understanding of the magnetic behavior of structures on this length scale is necessary in order to overcome the ''superparamagnetic limit'' that the technology will ultimately run into in its drive toward higher bit densities. Unfortunately, knowledge of nanoparticle materials cannot easily be deduced from knowledge of their bulk counterparts. Indeed, particle properties can, in some cases, be radically different[2] as increased magnetic moments due to enhanced spin and orbital contributions, as well as surface effects, can arise.[3] The aforementioned superparamagnetism, where thermal energy becomes greater than the anisotropy energy in a single-domain material resulting in a randomly fluctuating magnetic moment, is also common in materials on this scale.[4]

Aside from the nanoparticle properties themselves, interactions between nanoparticles arranged in arrays can be very important in determining the properties of a system. In the current investigation, nanoparticles were deposited onto a substrate such that the resulting array was disordered, with regions of clustering and regions containing single nanoparticles. These assemblies and their interactions were studied using atomic force microscopy (AFM) and magnetic force microscopy (MFM), the latter producing unusual observations which we hope to shed light on using a simple particle interaction model.

II. EXPERIMENTAL DETAILS

The iron nanoparticles used in this work consisted of 10.6 nm iron cores stabilized by the polymer polyisobutene (product name SAP 295). They were produced using the inverse micelle technique, in this case by thermally decomposing iron pentacarbonyl, $Fe(CO)_5$ in a decaline solution with the polymer.[5] The resulting polymer shell on the nanoparticles is approximately 10–12 nm thick, but is somewhat flexible, resulting in an average nanoparticle diameter of ~ 30 nm. Transmission electron microscopy images taken by the creators of the nanoparticles showed that the metal core consisted of two distinct regions. Subsequently, solutions of the nanoparticles were examined using Mössbauer spectroscopy,[6] which determined that these two regions consisted of oxide only, rather than iron and iron oxide.

Nanoparticle deposition was by means of the method described by Michelotto *et al.*[7] which involves placing a solution of the nanoparticles onto a substrate inclined at an angle within in a sealed container containing a vaporous atmosphere of the same solvent used for the nanoparticle solution. The resultant flow of the solution over the substrate results in an evenly distributed film of nanoparticles. In the present work, the method was effected by placing solvent-soaked tissue paper in the bottom of a petri dish containing a slightly inclined glass slide (in this case $\sim 10°$ with the horizontal) acting as a sample holder. An inverted petri dish was then used as a lid to contain the saturated atmosphere. In this way, a solution of the particles was deposited onto an inclined silicon substrate that was previously spin coated with the polymer Formvar to modify the nanoparticle surface adhesion (the degree of surface adhesion must not be too great

a)Electronic mail: fran.pedreschi@dit.ie

as the nanoparticles will then not flow over the surface, but it must also not be so low that they will not stick at all). This approach allows for slow controlled solvent evaporation and resulted in an evenly spread monolayer film.

The resulting samples consisting of a monolayer of iron nanoparticles were examined by AFM and MFM using a Digital Instruments Nanoscope IIIa. The tips used were commercial cantilevers from Digital Instruments, magnetic etched silicon probe type, with $L=225\,\mu$m, $F_o=71-100$ kHz. [8] The AFM topographic images were obtained in the tapping mode, whereas for the MFM images the so-called ''lift mode'' was applied.[9] This works by scanning a single line of the sample in topographic tapping mode using the magnetic tip, then applying the lift offset and performing a magnetic measurement. This is repeated line by line over the selected sample area. This removes any possibility that the particles are being moved by the tip, as it would be apparent when the tip performed its topographic scan on each successive line. The magnetic force gradient was measured in the frequency shift mode.[9]

III. RESULTS

Figures 1(a) and 1(b) show topographic and magnetic force gradient images, respectively, taken over the same region of the sample. Comparison of the two scans reveals an unusual effect: It can be seen that while individual nanoparticles are visible on both scans (square selections), nanoparticles gathered in clusters are strongly visible in the topographic image only (circle selections). On close observation, the magnetic force gradient image does show a slight cloudiness that appears to represent the perimeter region of the clusters. This ''cluster edge effect'' is just visible in the circle selections of Fig. 1(b), which was scanned at a lift height of 5 nm. Below this height, the van der Waals and capillary forces that comprise a topographic image were apparent in the magnetic images, and both AFM and MFM were very similar; and above 5 nm, the cluster edge effect was still observable but lateral resolution was diminished. The cloudiness is brighter on the left- of the clusters than on the right-hand side This is especially noticeable in the center of the circled region on the right-hand side of Fig. 1(b) which appears to be a gap between two closely spaced cluster formations. It was hypothesized that the cluster edge effect was likely due to a symmetry-breaking effect at the border of the cluster of nanoparticles. From magnetization measurements of these nanoparticles in solution,[6] it was evident that the blocking temperature is around 270 K.

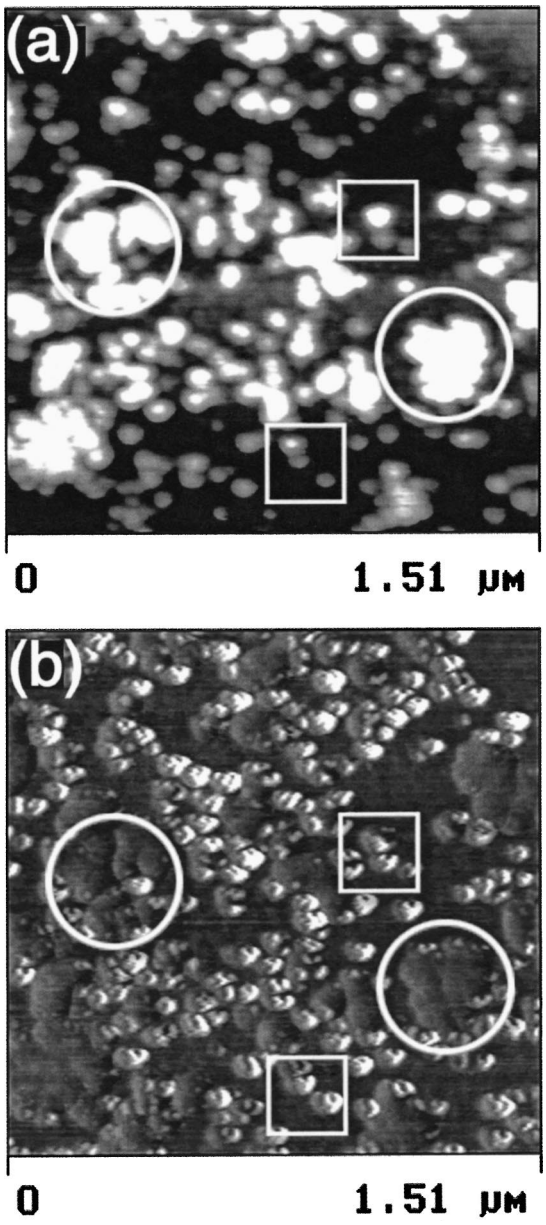

FIG. 1. (a) Topographic and (b) magnetic force gradient images of colloidal iron nanoparticles on a Formvar-coated SiO_2 substrate. Single particles are visible on both images (squares) while clusters are clearly visible on the topographic scan only (circles). A slight cloudiness, or cluster edge effect, appears to represent the perimeter region of the clusters in (b).

IV. ANALYSIS

In seeking to explain why the nanoparticle clusters give little MFM signal compared to isolated nanoparticles, two possible explanations can be considered. It was first hypothesized that the dipole interaction of the nanoparticles when arranged in clusters might be strong enough to prevent the nanoparticles from aligning with the tip as it passed over (as long as the tip is sufficiently high). Isolated particles with appreciable spacing from their neighbors would experience a weaker dipole interaction and be more easily aligned by the tip, which should therefore feel a greater force gradient. The cluster edge effect could be a manifestation of symmetry breaking at the edge of the cluster: The in-plane alignment of the moments in the clusters is disturbed due to the loss of symmetry at the edge, resulting in a more freely oriented magnetic moment of the outermost particles which have fewer nearest neighbors than those within the cluster. This, in turn, would then produce a larger force gradient between the tip and these outermost particles. An alternative explanation is that the weak local interactions produced by the particles in a cluster would not be strong enough to align them against the interaction of the tip, but would instead cause the formation of a spin glass system with a *random* distribution of dipoles. This would have almost no net magnetic field over

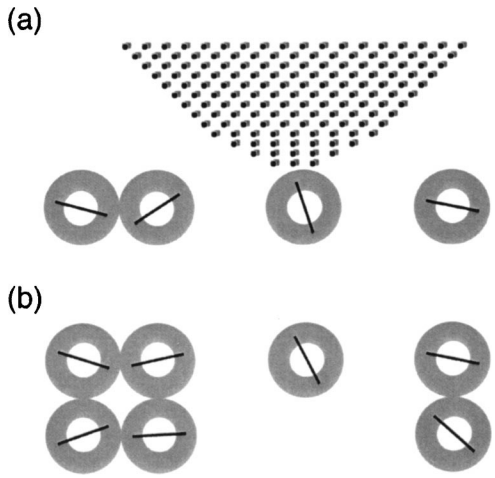

FIG. 2. A screen print of the model used for calculations in plane view (top) and elevation view (bottom). The tip is represented as a three-dimensional array of dipoles arranged into a rounded pyramid shape (small circles). The coated nanoparticles (large circles) form various structures such as four nanoparticles in a 2×2 cluster, two nanoparticles in a 1×2 cluster, and single isolated nanoparticles. Various distributions of such particles were tested.

the time scale of an MFM measurement, and therefore almost no interaction between the clusters and the tip would result. Again, the cluster edge may preferentially interact with the tip in this case due to a reduction in nearest neighbor count.

A model was developed in C++ using Borland C++ Builder 4 and calculations were performed to investigate the effects observed. The nanoparticles have ~10 nm iron cores and on this length scale should effectively be single domain and it is highly probable that they are superparamagnetic at room temperature. As the spacing between the cores is a minimum of ~30 nm due to the polymer coat, the interaction should be limited to dipolar only. The system was therefore modelled simply as a collection of interacting magnetic dipoles. The nanoparticles are described as large atoms and, therefore, they are described by a single dipole with a very low anisotropy. A sample was constructed consisting of seven particles: An arrangement of four nanoparticles in a 2×2 cluster, two nanoparticles in a 1×2 cluster, and a single isolated nanoparticle, as shown in Fig. 2. This arrangement serves to illustrate the contrast between single nanoparticles and clusters. The cluster sizes in the experimental MFM image are sometimes larger, but the effect manifests itself in clusters of two nanoparticles and more, as long as the constituent nanoparticles are closely spaced. Although the polymer coat, which is slightly flexible, might allow the particles to be a bit closer than 30 nm, such variation cannot be adequately characterized from the experimental MFM images so 30 nm was chosen as the fixed particle separation in the clusters.

The particle anisotropy takes the form of a constant applied magnetic field of random orientation for each particle. This has a simple cosine dependence, whereas the anisotropy of a uniaxial superparamagnetic particle, in fact, has a cosine squared dependence. There was no easy way to put this cosine squared dependence into the model. In practice, it was found that the difference between low and zero anisotropy, in the form in which is applied here, was negligible and mostly not observable at all. Of course, given that the dependency of the anisotropy is incorrect, this may have no real meaning. For these reasons, the anisotropy was actually set to zero in the calculations.

The tip is modeled as a three-dimensional array of dipoles arranged into a rounded pyramid shape, as shown in Fig. 2. The magnetic moment of each tip dipole is fixed in value and direction, pointing vertically downward. These elements do not interact with each other during calculations. The nanoparticle dipoles are allowed to interact with each other and with the tip dipoles. The separation between dipoles in the tip is 8 nm in the x, y, and z directions. This has no correspondence to the actual tip domain sizes, but allows reasonably accurate modelling of the shape of the tip. The measured magnetization of the tip was spread over these dipoles, so the actual magnetization of each tip dipole is calculated dynamically, depending on the number of dipoles in the chosen tip size. In practice, tips with approximately 3×10^4 dipole elements were used, corresponding to a pyramid with a length of side of around 350 nm. While this is smaller than the real tip dimensions, it was found to be unnecessary to use larger tips in the model as they had no obvious effect on the image and considerably slowed calculation time.

Each nanoparticle, at position $\mathbf{r}$, is initialized with a user-defined magnetic moment $\mathbf{m}$ of random orientation. Initially, the $\mathbf{H}$ field generated at each nanoparticle center by the tip is calculated using Eq. (1), summing over all tip elements,

$$\mathbf{H}_i=\frac{3(\mathbf{m}.\mathbf{r})r_i-m_i r^2}{4\pi r^5},\ i=x,y,z. \tag{1}$$

This field is then used to calculate the nanoparticle magnetization using the Langevin function, Eq. (2), which allows a form of temperature dependence to be included in the model: (The temperature was set to 298 K for the purposes of the Langevin function)

$$M=M_s\left[\coth\left(\frac{\mu H}{kT}\right)-\left(\frac{kT}{\mu H}\right)\right]. \tag{2}$$

The interactions of the nanoparticles are now considered, with the $\mathbf{H}$ field at each nanoparticle center being calculated by summing the interactions from all the other nanoparticles. This $\mathbf{H}$ field is added to the tip-induced field to produce an overall field, and the magnetic moment of the nanoparticles is then recalculated. The magnetic energy of the system is also calculated at this point. The calculation then iterates, using the calculated nanoparticle magnetization to recalculate the $\mathbf{H}$ field at each nanoparticle. The magnetic energy is compared after each iteration, and the loop exits when this is minimized. The nanoparticle states are then reinitialized, and the process is repeated so that several random starting points are considered. The final lowest-energy state is selected and the force is evaluated between the tip and sample dipole, summing these interactions over all dipoles in the system. The tip is then moved vertically over a predetermined distance, corresponding to the oscillation amplitude, and the

calculation procedure is repeated, allowing the force gradient to be calculated. The tip is then moved over the sample surface in the $x-y$ plane and the force gradient is calculated at each point. The result is then represented in an image form that can be compared to the experimental data.

This rather simple model ignores the effect of van der Waals forces which can influence topographic AFM interactions and capillary forces which occur due to a layer of adsorbed moisture that can bridge the tip and sample in ambient AFM. However, both forces are marginal at the chosen tip–sample separation and so their effect can be considered negligible.[10]

The lift height was set to 5 nm with an oscillation amplitude of 2 nm (i.e., ± 1 nm from the equilibrium position of the tip). The quantity μ, the magnetic dipole moment was taken from Ref. 11 to be 6.32×10^{-19} A m^2, where magnetic hysteresis measurements were fitted to the Langevin function to estimate μ for two interacting hemispherical iron particles. Although the Mössbauer study suggested that the nanoparticles in this case were iron oxide, not iron, it is the closest indicator to a possible value for particles of a similar size to those used in these experiments. Consideration of the average nanoparticle volume for a radius of 10 nm and the bulk magnetization of iron (1707×10^3 A/m) gives an upper limit of approximately 9×10^{-19} A m^2 for the magnetic dipole moment of the nanoparticles, considering that oxide formation is present. This is consistent with values used here. It seems, in general, that μ may be four or five orders of magnitude greater than the atomic value.[11,12] The tip magnetization was set to 400,000 A m during all calculations, which was experimentally determined for the tips used here following the same procedure as that outlined by Carl *et al.*[13] This agrees reasonably with magnetizations used in calculations of other ferromagnetic materials.[14] The tip shape was rounded with a radius approximating 25 nm, which matched the tip specifications. The nanoparticle saturation magnetization was then varied and force gradient images were obtained.

Figure 3 shows the results of these simulations. The force gradients were of the order of 10^{-3} N/m. As the saturation magnetization of the nanoparticles is varied from 1×10^5 to 1×10^6 A m the response of the isolated nanoparticles becomes prominent in the images as the interaction of the nanoparticles in the clusters reduces their influence on the MFM tip. These images are similar to the experimental MFM images, although the resolution is noticeably lower. The progression from a dominant cluster response to a dominant single nanoparticle response can be seen in the transition from Figs. 3(a) to 3(c). A slight edge effect is also visible around the clusters, consistent with expectations, although not as prominent as that visible in the experimental MFM image of Fig. 1(b). The effect of instrument resolution was also studied by reducing the tip radius to 10 nm, although this is an impractical value for commercial tips at present. There was more lateral contrast in the resulting images but, otherwise, the images were unchanged.

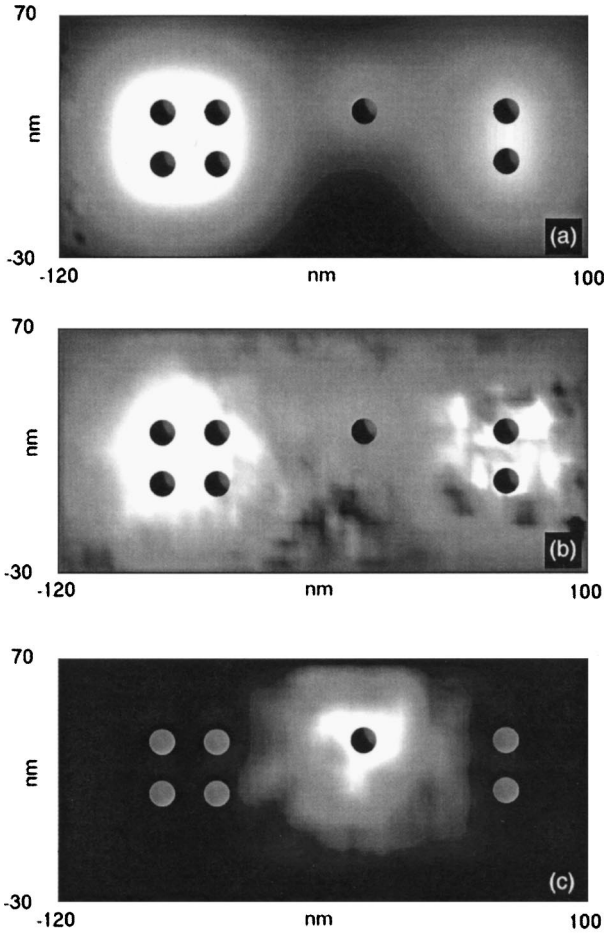

FIG. 3. Simulations of the interaction of an MFM tip with the various types of particle cluster considered. M_s for the tip is about 4×10^5 A m throughout. The images represent particle M_s values of (a) 1×10^5 A m, (b) 5×10^5 A m, and (c) 1×10^6 A m. The progression shows the increasing prominence of the single particle. The particle positions are indicated by dots.

V. DISCUSSION

The authors are well aware that any system, such as this, is likely to be quite complex and that the present model is insufficient to solve the system in any great detail. The aim here was to produce a simple, largely qualitative, model that would give insight into the *general* behavior and trends in such a system, where the MFM results were clearly unusual. This goal has been achieved in that the simple model used here did produce images similar to those observed with MFM. Which of the proposed hypotheses for the observations is correct, interparticle interaction within clusters or spin glass formation, is less clear. Both effects would likely produce similar images in MFM studies.

If the tip is removed from the calculation, by setting the magnitude of all its dipoles to zero, the particles always attain a state of random spin distribution, which appears to have no pattern with successive reinitializations of the system. When the tip is present, the particle dipoles at first glance seem to also fall into a random distribution, but while reinitializing the model does produce a different dipole distribution, it is not as pronounced as the variation obtained in the absence of the tip. There seems to be a degree of under-

lying order, which depends on the position of the tip, and increases in magnitude if the magnetization of the tip is increased. It does remain some way short of the total ordering that would be expected from the first hypothesis, but is not the completely random behavior expected of a spin glass either—it appears to be somewhere in between.

Despite the qualitative success, the model clearly has some significant limitations. A number of arbitrary assumptions are made about the particle properties and those that need to be considered or neglected, for example, there is no consideration of the internal structure of the particle. Although internal structure is very important in determining the exact behavior of a particle and the origin of the unusual properties, one can argue that the MFM responds to dipolar forces which are relatively long range and is, therefore, largely incapable in its current form of imaging internal structure. This, in itself, does not justify the absence of internal effect considerations but the single domain superparamagnetic character and the presence of the polymer shell, which limits interparticle interactions to dipolar, constitute reasonable justification.

A greater problem is the form of the magnetic anisotropy. Calculations were initially carried out with fields of 1 to 10 A m. It was found that this variation had little effect on the generated images, and higher anisotropy seemed to induce an instability in the calculations, requiring more iterations to reach the energy minimum which, in some cases, dramatically increased calculation time. Setting the anisotropy to zero also had no effect on the generated images, but slightly reduced the instability. For that reason, images generated with zero anisotropy are presented here. It was noted that increasing the anisotropy tended to reduce the ability of the tip to align the isolated particle, making the images in 3(b) and 3(c) more difficult to obtain. This would be expected, as increasing the anisotropy reduces the superparamagnetic behavior of the particles. In addition it would be expected that the external field is larger than the anisotropy field. It may then be assumed, at least for particles close to the tip, that the internal anisotropy has little significance. Although this seems to be a somewhat circular argument, in that the angular dependency of the anisotropy used here is incorrect to begin with, it is hoped that the argument still has validity. Certainly, the reproducibility of the images would seem to suggest this.

The final impression is that the model used is very simple, while the system being modeled is so complex that complete theoretical treatment is not currently attainable. Despite this, the model does give very good agreement with the MFM data though it is still not conclusive in determining the underlying reason for the observed effects. It suggests that the cluster particles may be forming a spin glass-type system, but with a slight degree of ordering caused in the presence of the magnetic tip. Further investigations are underway, both experimentally and computationally, to help elucidate this issue.

ACKNOWLEDGMENTS

The authors appreciate discussions with Coen Swüste with regard to the **H** field calculations. They also acknowledge the Radiation Physics Group in Delft University of Technology for performing Mössbauer experiments on the iron particles. Two of the authors (F.P. and J.D.O'M.) acknowledge support from the Enterprise Ireland International Collaboration program and from the Facility for Optical Characterization and Spectroscopy (FOCAS) at the Dublin Institute of Technology, which is funded under the National Development Plan 2000 to 2006 with assistance from the European Regional Development Fund.

[1] See, for example, *Quantum Physics of Atoms, Molecules, Solids, Nuclei, and Particles*, edited by R. Eisberg and R. Resnick, 2nd ed. (Wiley, New York, 1985).
[2] *Magnetic Properties of Fine Particles*, edited by J. L. Dormann and D. Fiorani (North–Holland, Amsterdam, 1992).
[3] M. Tischer, O. Hjortstam, D. Arvanitis, J. Hunter Dunn, F. May, K. Baberschke, J. Trygg, J. M. Wills, B. Jahansson, and O. Eriksson, Phys. Rev. Lett. **75**, 1602 (1995).
[4] For example, S. Yamamuro, K. Sumiyama, T. Kamiyama, and K. Suzuki, J. Appl. Phys. **86**, 5726 (1999).
[5] C. Pathmamanoharan and A. P. Philipse, J. Colloid Interface Sci. **205**, 340 (1998).
[6] C. Pathmamanoharan, Ph.D. thesis, University of Utrecht, ISBN 90-393-1575-2 (1998).
[7] R. Micheletto, H. Fukuda, and M. Ohtsu, Langmuir **11**, 3333 (1995).
[8] http://www.ssp.gla.ac.uk/Reports/MFM_characterisation.htm.
[9] Digital Instruments, Scanning Probe Microscope Manuals, Santa Barbara, Ca. Chaps. 8,11,13
[10] T. Stifter, O. Marti, and B. Bhushan, Phys. Rev. B **62**, 13667 (2000).
[11] Y. Park, S. Adenwalla, G. P. Felcher, and S. D. Bader, Phys. Rev. B **52**, 12779 (1995).
[12] M. F. Hansen and S. Mørup, J. Magn. Magn. Mater. **184**, 262 (1998).
[13] A. Carl, J. Lohau, S. Kirsch, and E. F. Wassermann, J. Appl. Phys. **89**, 6098 (2001).
[14] M. Kleiber, F. Kümmerlen, M. Löhndorf, A. Wadas, D. Weiss, and R. Wiesendanger, Phys. Rev. B **58**, 5563 (1998).